Article
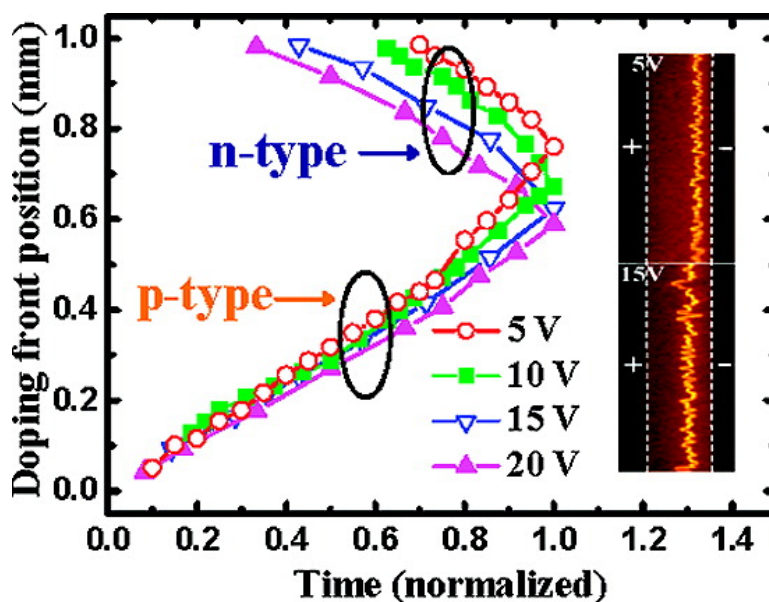
Identifying and Alleviating Electrochemical Side-Reactions in Light-Emitting Electrochemical Cells

Junfeng Fang, Piotr Matyba, Nathaniel D. Robinson, and Ludvig Edman

More About This Article

Additional resources and features associated with this article are available within the HTML version:

- Supporting Information
- Links to the 2 articles that cite this article, as of the time of this article download
- Access to high resolution figures
- Links to articles and content related to this article
- Copyright permission to reproduce figures and/or text from this article

View the Full Text HTML

Identifying and Alleviating Electrochemical Side-Reactions in Light-Emitting Electrochemical Cells

Junfeng Fang,[†] Piotr Matyba,[†] Nathaniel D. Robinson,[‡] and Ludvig Edman*,[†]

Department of Physics, Umeå University, SE-901 87 Umeå, Sweden and Department of Science and Technology, Linköping University, SE-601 74 Norrköping, Sweden

Received December 27, 2007; E-mail: ludvig.edman@physics.umu.se

Abstract: We demonstrate that electrochemical side-reactions involving the electrolyte can be a significant and undesired feature in light-emitting electrochemical cells (LECs). By direct optical probing of planar LECs, comprising Au electrodes and an active material mixture of {poly[2-methoxy-5-(2-ethylhexyloxy)-1,4-phenylenevinylene] (MEH-PPV) + poly(ethylene oxide) (PEO) + KCF$_3$SO$_3$}, we show that two direct consequences of such a side-reaction are the appearance of a "degradation layer" at the negative cathode and the formation of the light-emitting p–n junction in close proximity to the cathode. We further demonstrate that a high initial drive voltage and a high ionic conductivity of the active material strongly alleviate the extent of the side reaction, as evidenced by the formation of a relatively centered p–n junction, and also rationalize our findings in the framework of a general electrochemical model. Finally, we show that the doping concentrations in the doped regions at the time of the p–n junction formation are independent of the applied voltage and relatively balanced at ∼0.11 dopants/MEH-PPV repeat unit in the p-type region and ∼0.15 dopants/MEH-PPV repeat unit in the n-type region.

Introduction

Conjugated polymers (CPs) are currently attracting great interest for use in various applications, e.g., field-effect transistors,[1–4] solar cells,[5–8] and data-storage devices,[9–14] due to a set of unique and appealing properties; these include straightforward design of the chemical structure, tuneable conductivity, efficient absorption and fluorescence, low fabrication cost, and mechanical flexibility. For light-emitting applications, two main types of CP-based devices have emerged: the polymer light-emitting diode (PLED)[15–19] and the light-emitting electrochemical cell (LEC).[20–36] The main difference between these two devices is that the LEC contains a solid-state electrolyte admixed with the CP in the active material, which facilitates its initial electrochemical operation, while the PLED is an entirely electronic device.

* To whom correspondence should be addressed. Tel: +46-90-786 5732. Fax: +46-90-7866673. E-mail: ludvig.edman@physics.umu.se.

† Department of Physics, Umeå University.

‡ Department of Science and Technology, Linköping University.

(1) Garnier, F.; Hajlaoui, R.; Yassar, A.; Srivastava, P. *Science* **1994**, *265*, 1684–1686.
(2) Dzwilewski, A.; Wågberg, T.; Edman, L. *Phys. Rev. B.* **2007**, *75*, 075203.
(3) Takashima, W.; Murasaki, T.; Nagamatsu, S.; Morita, T.; Kaneto, K. *Appl. Phys. Lett.* **2007**, *91*, 071905.
(4) Andersson, L. M.; Inganäs, O. *Org. Electron.* **2007**, *8*, 423–430.
(5) Sariciftci, N. S.; Smilowitz, L.; Heeger, A. J.; Wudl, F. *Science* **1992**, *258*, 1474 -1476.
(6) Tvingstedt, K.; Andersson, V.; Zhang, F.; Inganäs, O. *Appl. Phys. Lett.* **2007**, *91*, 123514.
(7) Zhang, Y. G.; Hu, Y. F.; Gao, J. *Appl. Phys. Lett.* **2007**, *91*, 233509.
(8) Perzon, E.; Zhang, F. L.; Andersson, M.; Mammo, W.; Inganäs, O.; Andersson, M. R. *Adv. Mater.* **2007**, *19*, 3308–3311.
(9) Moller, S.; Perlov, C.; Jackson, W.; Taussig, C.; Forrest, S. R. *Nature* **2003**, *426*, 166–169.
(10) Ouyang, J. Y.; Chu, C. W.; Szmanda, C.; Ma, L. P.; Yang, Y. *Nat. Mater.* **2004**, *3*, 918–922.
(11) Ling, Q.; Song, Y.; Ding, S. J.; Zhu, C.; Chan, D. S. H.; Kwong, D. L.; Kang, E. T.; Neoh, K. G.; *Adv. Mater.* **2005**, *17*, 455–459.
(12) Verbakel, F.; Meskers, S. C. J.; Janssen, R. A. J. *Chem. Mater.* **2006**, *18*, 2707–2712.
(13) Patil, S.; Lai, Q. X.; Marchioni, F.; Jung, M. Y.; Zhu, Z. H.; Chen, Y.; Wudl, F. *J. Mater. Chem.* **2006**, *16*, 4160–4164.
(14) Jakobsson, F. L. E.; Crispin, X.; Colle, M.; Buchel, M.; de Leeuw, D. M.; Berggren, M. *Org. Electron.* **2007**, *8*, 559–565.
(15) Burroughs, J. H.; Bradley, D. D. C.; Brown, A. R.; Marks, R. N.; Mackay, K.; Friend, R. H.; Bums, P. L.; Holmes, A. B. *Nature* **1990**, *347*, 539–541.
(16) Burn, P. L.; Holmes, A. B.; Kraft, A.; Bradley, D. D. C.; Brown, A. R.; Friend, R. H.; Gymer, R. W. *Nature* **1992**, *356*, 47–49.
(17) Hoven, C.; Yang, R.; Garcia, A.; Heeger, A. J.; Nguyen, T. Q.; Bazan, G. C. *J. Am. Chem. Soc.* **2007**, *129*, 10967–10977.
(18) Tavasli, M.; Bettington, S.; Perepichka, I. F.; Batsanov, A. S.; Bryce, M. R.; Rothe, C.; Monkman, A. P. *Eur. J. Inorg. Chem.* **2007**, *30*, 4808–4814.
(19) Garcia, A.; Yang, R.; Jin, Y.; Walker, B.; Nguyen, T. Q. et al. *Appl. Phys. Lett.* **2007**, *91*, 153502.
(20) Pei, Q. B.; Yu, G.; Zhang, C.; Yang, Y.; Heeger, A. J. *Science* **1995**, *269*, 1086–1088.
(21) Pei, Q. B.; Yu, G.; Zhang, C.; Yang, Y.; Heeger, A. J. *J. Am. Chem. Soc.* **1996**, *118*, 3922–3929.
(22) Gao, J.; Yu, G.; Heeger, A. J.; *Appl. Phys. Lett.* **1997**, *71*, 1293–1295.
(23) Yu, G.; Cao, Y.; Andersson, M.; Gao, J.; Heeger, A. J. *Adv. Mater.* **1998**, *10*, 385–388.
(24) deMello, J. C.; Tessler, N.; Graham, S. C.; Friend, R. H. *Phys. Rev. B.* **1998**, *57*, 12951–12963.
(25) Johansson, T.; Mammo, W.; Andersson, M. R.; Inganas, O. *Chem. Mater.* **1999**, *11*, 3133–3139.
(26) Tasch, S.; Gao, J.; Wenzl, F. P.; Holzer, L.; Leising, G.; Heeger, A. J.; Scherf, U.; Mullen, K. *Electrochem. Solid. State. Lett.* **1999**, *2*, 303–305.
(27) Wilson, J. S.; Frampton, M. J.; Michels, J.; Sardone, L.; Marletta, G.; Friend, R. H.; Samorì, P.; Anderson, H. L.; Cacialli, F. *Adv. Mater.* **2005**, *17*, 2659.
(28) Leger, J. M.; Carter, S. A.; Ruhstaller, B. *J. Appl. Phys.* **2005**, *98*, 124907.
(29) Habrard, F.; Ouisse, T.; Stephan, O. *J. Phys. Chem. B.* **2006**, *110*, 15049–15051.
(30) Simon, D. T.; Stanislowski, D. B.; Carter, S. A. *Appl. Phys. Lett.* **2007**, *90*, 103508.
(31) Yim, Y. C.; Park, J. H.; Kim, S. W.; Choi, E. H.; Cho, G. S.; Seo, Y. H.; Kang, S. O.; Park, B.; Cho, S. H.; Kim, I. T.; Han, S. H.; Lim, J.; Takezoe, H. *Appl. Phys. Lett.* **2006**, *89*, 103507.

Recent PLEDs have demonstrated impressive performance, but two notable drawbacks with these devices are that a low work-function (and reactive) metal cathode and a very thin (and pinhole-prone) active layer are required for satisfactory operation. In contrast, LECs can be operated in an efficient manner in device configurations comprising air-stable metals for both electrodes and a thick active material. A notable example of these important advantages is the recently reported planar LECs ("surface cells"), comprising two identical Au electrodes separating a mm-thick active material, which emit significant light at a low applied voltage.[37−38] However, despite these attractive features, LECs have so far attracted very limited commercial interest, partially because their operational lifetime has not reached commercial standards yet.[39−47]

In order to address and resolve the operational stability problem and to attain an optimal device performance, we are working with the identification and alleviation of chemical and electrochemical side-reactions in LECs.[48] In this work, we have utilized a planar surface cell structure, with an active material of {MEH-PPV + PEO + KCF$_3$SO$_3$} and with an extremely large (mm-scale) inter-electrode gap separating two Au electrodes. Figure 1a presents the chemical structures of the active material components, and Figure 1, parts b and c, presents schematics of the planar device configuration. We demonstrate that an electrochemically induced "side-reaction"—specifically, an irreversible reduction of the solid-state electrolyte at the negative cathode—can be the dominant cathodic electrochemical process in such common LECs during the initial electrochemical operation. Two direct and important consequences of this side-reaction are that the position of the light-emitting p−n junction in the inter-electrode gap is strongly dependent on the operational conditions, and that a degradation layer is formed at the negative Au cathode. Furthermore, we provide some general operational guidelines for how to minimize this undesired side-reaction, and we show that these result in a desired centered p−n junction and the absence of the degradation layer. A centered p−n junction is attractive because it minimizes the risks for doping-induced micro shorts[45] and electrode-induced quenching of the light emission. Finally, we rationalize our
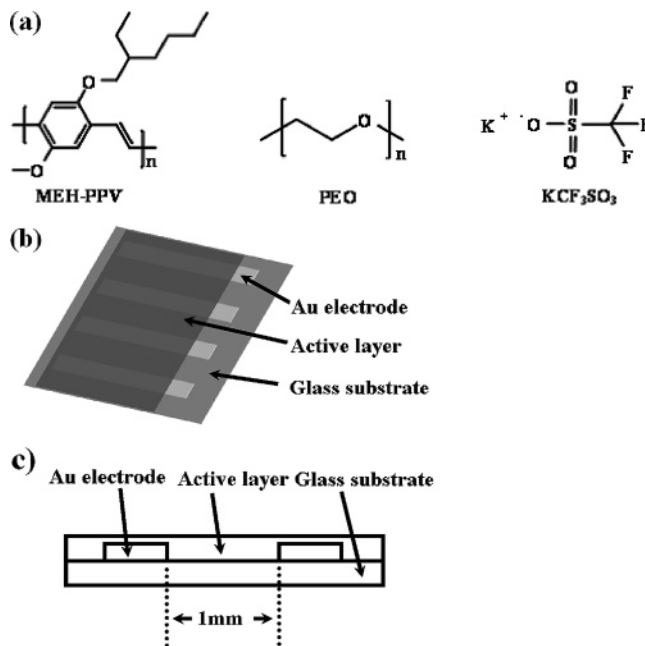
Figure 1. (a) Chemical structures of the components in the {MEH-PPV + PEO + KCF$_3$SO$_3$} active material. (b) The employed device architecture showing three planar devices on a glass substrate in a top view, and (c) a schematic showing the cross-sectional view of one planar device with a 1 mm inter-electrode gap.

findings in the context of a straightforward electrochemical model.

Experimental Section

Poly[2-methoxy-5-(2-ethyl-hexyloxy)-1,4-phenylenevinylene] (MEH-PPV, Aldrich, M_n = 40000−70000 g/mol) was used as received. Poly-(ethylene oxide) (PEO, M_w = 5 × 10^6, Aldrich) and the salt KCF$_3$SO$_3$ (98%, Alfa Aesar) were dried at a temperature (T) of 323 K and 473 K, respectively, under vacuum. Master solutions of 10 mg/mL concentration were prepared: MEH-PPV dissolved in chloroform (>99%, anhydrous, Aldrich), and PEO and KCF$_3$SO$_3$ dissolved separately in cyclohexanone (99%, Merck). A blend solution was prepared by mixing the master solutions together in a mass ratio of MEH-PPV:PEO:KCF$_3$SO$_3$ = 1:1.35:0.25, followed by stirring on a magnetic hot plate at T = 323 K for at least 5 h. The 1.5 × 1.5 cm^2 glass substrates were cleaned by subsequent ultrasonic treatment in detergent, acetone, and isopropanol solutions. The 100-nm-thick Au electrodes were deposited onto the cleaned glass substrates by thermal evaporation at p < 2 × 10^{-4} Pa. The inter-electrode gap was established by an Al shadow mask.

The blend solution was deposited by spin-coating at 800 rpm for 60 s, which resulted in active material films with a thickness of 150 nm. The films were thereafter dried on a hot plate at T = 333 K for at least 5 h. Finally, immediately preceding a measurement, in situ drying in the cryostat for 2 h at T = 360 K and under vacuum (p < 10^{-3} Pa) took place. All of the above device preparation procedures, with the exception of the cleaning of substrates were carried out in an Ar-filled glove box (O$_2$ < 3 ppm, H$_2$O < 0.5 ppm). The characterization of devices was performed under vacuum (p < 10^{-3} Pa) in an optical-access cryostat. A computer-controlled source-measure unit (Keithley 2400) was employed to apply voltage and to measure the resulting current. The photographs of the doping progression were recorded under UV (λ = 365 nm) illumination through the optical window of the cryostat, using a digital camera (Cannon EOS 20D) equipped with a macro lens.

Cyclic voltammetry (CV) measurements were carried out with a computer-controlled potentiostat/galvanostat (Autolab, PGSTAT302/FRA2, Eco Chemie) using the General Purpose Electrochemical

(32) Hu, Y. F.; Gao, J. *Appl. Phys. Lett.* **2006**, *89*, 253514.
(33) Leger, J. M.; Rodovsky, D. B.; Bartholomew, G. P. *Adv. Mater.* **2006**, *18*, 3130−3134.
(34) Su, H. C.; Fang, F. C.; Hwu, T. Y.; Hsieh, H. H.; Chen, H. F.; Lee, G. H.; Peng, S. M.; Wong, K. T.; Wu, C. C. *Adv. Funct. Mater.* **2007**, *17*, 1019−1027.
(35) Wenzl, F. P.; Fian, A.; Polt, P.; Rudorfer, A.; Leising, G. *Electrochim. Acta* **2007**, *52*, 6229−6236.
(36) Sax, S.; Mauthner, G.; Piok, T.; Pradhan, S.; Scherf, U.; List, E. J. W. *Org. Electron.* **2007**, *8*, 791−795.
(37) Shin, J. H.; Dzwilewski, A.; Iwasiewicz, A.; Xiao, S.; Fransson, A.; Ankah, G. N.; Edman, L. *Appl. Phys. Lett.* **2006**, *89*, 013509.
(38) Shin, J. H.; Edman, L. *J. Am. Chem. Soc.* **2006**, *128*, 15568−15569.
(39) Kervella, Y.; Armand, M.; Stephan, O. *J. Electrochem. Soc.* **2001**, *148*, H155−H160.
(40) Edman, L.; Moses, D.; Heeger, A. J. *Synth. Met.* **2003**, *138*, 441- 446.
(41) Shin, J. H.; Xiao, S.; Fransson, A.; Edman, L. *Appl. Phys. Lett.* **2005**, *87*, 043506.
(42) Zhang, Y.; Gao, J. *J. Appl. Phys.* **2006**, *100*, 084501.
(43) Bolink, H. J.; Cappelli, L.; Coronado, E.; Graetzel, M.; Orti, E.; Costa, R.; Viruela, P. M.; Nazeeruddin, Md. K. *J. Am. Chem. Soc.* **2006**, *128*, 14786−14787.
(44) Robinson, N. D.; Shin, J. H.; Berggren, M; Edman, L. *Phys. Rev. B* **2006**, *74*, 155210.
(45) Shin, J. H.; Robinson, N. D.; Xiao, S.; Edman, L. *Adv. Funct. Mater.* **2007**, *17*, 1807−1813.
(46) Slinker, J. D.; Rivnay, J.; Moskowitz, J. S.; Parker, J. B.; Bernhard, S.; Abruna, H. D.; Malliaras, G. G. *J. Mater. Chem.* **2007**, *17*, 2976−2988.
(47) Shao, Y.; Bazan, G. C.; Heeger, A. J. *Adv. Mater.* **2007**, *19*, 365−370.
(48) Wågberg, T.; Hania, P. R.; Robinson, N. D.; Shin, J. H.; Matyba, P.; Edman. L. *Adv. Mater.,* in press.
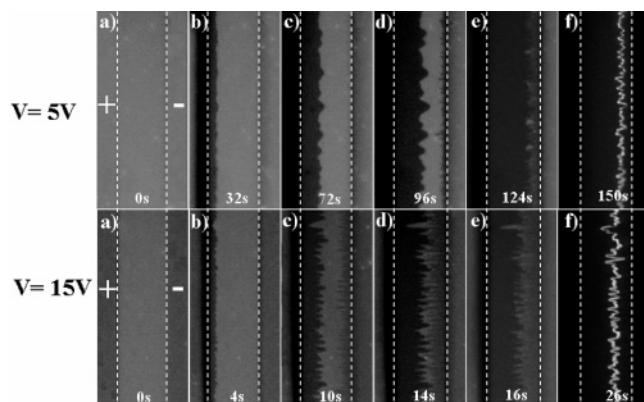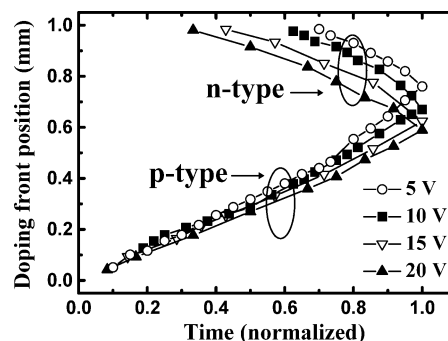
Figure 2. Doping front propagation and subsequent light emission in planar Au/ {MEH-PPV + PEO + KCF$_3$SO$_3$}/Au surface cells with a 1 mm inter-electrode gap during operation at $T = 360$ K and $V = 5$ V (top panel) and $V = 15$ V (bottom panel), respectively. The time of applied voltage is indicated in the bottom part of each photograph.

Figure 3. Average positions of the p-type and the n-type doping front, respectively, as a function of time (normalized to the time at which the p−n junction forms) for planar Au/{MEH-PPV + PEO + KCF$_3$SO$_3$}/Au surface cells with a 1-mm inter-electrode gap during operation at various applied voltages.

Software (GPES, Eco Chemie). All of the measurements were performed in an Ar-filled glove box (O$_2$ < 3 ppm, H$_2$O < 0.5 ppm). The electrolyte solution was either 0.1 M tetrabutylammonium hexafluorophosphate (TBAPF$_6$, ≥ 99.0%, Fluka) in acetonitrile (CH$_3$CN, anhydrous, ≥ 99.8%, Aldrich) or 0.1 M potassium trifluoromethanesulfonate (KCF$_3$SO$_3$, 98%, Alfa Aesar) and 2 M (calculated as a number of repeat units of PEO per L of solution) low-molecular-weight PEO ($M_w = 400$, Polysciences) in acetonitrile. Au working electrodes were deposited onto pre-cleaned glass substrates by thermal evaporation at $p < 2 \times 10^{-4}$ Pa. MEH-PPV films were spin-coated from the chloroform solution (10 mg/mL, > 99%, anhydrous, Aldrich) onto the Au electrodes at 800 rpm for 60 s and thereafter dried on a hot plate at $T = 323$ K for ~1 h. A silver wire was used as the quasi-reference electrode. The silver wire was calibrated vs the bis-(η-cyclopentadienyl)-iron(II)/ bis-(η-cyclopentadienyl)iron(II)$^+$ ion (ferrocene/ferrocenium ion, Fc/Fc$^+$) reference redox couple (ferrocene, ≥ 98%; Fluka) at the end of each measurement by adding ~10^{-5} mol of ferrocene into the electrolyte solution and performing a sweep. A Pt rod was used as the counter electrode. The reduction/oxidation onset potentials were defined to correspond to the crossing point between the baseline and the half-peak-height tangent line. All the potentials are reported vs the Fc/Fc$^+$ reference redox couple.

Results and Discussion

The initial operation of LECs involves electrochemical doping, which transforms the CP from being essentially an electronic insulator (in the undoped state) to a good conductor (in the doped state).[49−52] Ideally, the CP is electrochemically p-type doped at the positive anode, via injection of holes and subsequent electrostatic compensation by anions, and n-type doped at the negative cathode, via injection of electrons and compensation of cations. During this initial electrochemical doping process, p-type and n-type doping fronts progress toward each other in the inter-electrode gap until a light-emitting p-n junction is formed. The entire turn-on process of a LEC device can be conveniently visualized under UV illumination in a dark room, since the strong UV-excited photoluminescence of many CPs (e.g., MEH-PPV) is effectively quenched by doping.

Figure 2 presents sequences of photographs of the doping front progression and the subsequent light emission for two representative planar Au/{MEH-PPV + PEO + KCF$_3$SO$_3$}/Au

surface cell devices with a 1-mm inter-electrode gap. The positive anode is positioned to the left in the photographs. The doped regions appear as dark areas originating at the electrode interfaces (marked with dashed lines). The device presented in the upper panel of photographs was biased at $V = 5$ V, and the device presented in the lower panel was biased at $V = 15$ V. The presented photographs were selected such that the p-type doping front had progressed the same distance in the inter-electrode gap in the two photographs marked with the same letter.

From Figure 2, it is clear that the n-type doping onset, compared to the p-type doping onset, is delayed in both devices; see the two photographs (b), where p-type doping but not n-type doping is apparent. Moreover, this delay of the n-type doping onset is significantly more prominent in the device biased at $V = 5$ V, as seen in the first signs of n-type doping already in photograph (c) in the device biased at $V = 15$ V but only in photograph (d) in the device biased at $V = 5$ V. The delay of the n-type doping onset has the direct consequence that the light-emitting p−n junction is formed closer to the negative cathode in the device biased at $V = 5$ V (see photographs e and f).

Two other interesting and consistent observations in all the devices investigated (>40 in total) concern the shape of the doping front. First, the shape of the p-type front becomes more jagged with time and with increasing voltage, which is a direct consequence of the ion-transport limited turn-on process (see ref 44 for an explicit discussion on this issue). Second, and more relevant to this study, the initial n-type front exhibits a spike-like appearance that is absent in the initial p-type front. We will return to this issue later in this paper.

Figure 3 presents the average positions of the p-type doping front and the n-type doping front as a function of time (normalized to the time at which the p−n junction forms) at various applied voltages. Three general trends are apparent: (i) the onset time for p-type doping is essentially independent of the applied voltage; (ii) the delay in the n-type doping onset is more significant at lower applied voltage; and (iii) the average position of the light-emitting p−n junction (as observed at time = 1.0) is shifted toward the negative cathode with decreasing applied voltage, from 0.59 mm away from the positive anode in devices with a 1-mm inter-electrode gap at $V = 20$ V to 0.76 mm at $V = 5$ V.

(49) Gao, J.; Heeger, A. J.; Campbell, I. H.; Smith, D. L. *Phys. Rev. B.* **1999**, *59*, R2482−R2485.
(50) Gao, J.; Dane, J. *Appl. Phys. Lett.* **2004**, *84*, 2778−2780.
(51) Edman, L. *Electrochim. Acta.* **2005**, *50*, 3878−3885.
(52) Hu, Y. F.; Tracy, C.; Gao, J. *Appl. Phys. Lett.* **2006**, *88*, 123507.

We observe a similar behavior with decreasing temperature, as we find that the delay in the n-type doping onset, as compared to the p-type doping onset, increases significantly and that the p−n junction shifts cathodically at lower temperatures (data not shown). Since it is well-established that these active materials exhibit a strongly temperature-dependent ionic conductivity,[37,53−55] we attribute the increasing delay in the n-type doping onset, and the resulting cathodic shift of the p−n junction, to reduced ionic conductivity. Importantly, the observed shift of the light-emitting p−n junction toward the center of the interelectrode gap for devices operated at high applied voltage and with highly ion-conducting active material is expected to have positive implications for device performance, since it will, for example, effectively eliminate problems with metal-induced quenching of the light emission and doping induced short-circuit formation, particularly in thin sandwich cells.[56−58]

In two previous publications,[45,59] we have presented a method for calculating the concentration of dopants in the p- and n-type doping regions at the time of the p−n junction formation. The method makes use of the fact that balanced oxidation and reduction takes place at the anodic and cathodic interfaces, respectively, in LECs during the turn-on process (since it is a solely electrochemical device during device turn-on); and that accordingly, an integration of the current up to the time for the p−n junction formation (as visually detected in planar devices) yields the total oxidation/reduction charge injected at each interface. If one then makes the assumption that all oxidation/reduction charge goes to electrochemical p-type/n-type doping of the CP, then calculating the concentration of dopants in the p-type/n-type region simply requires dividing the total oxidation/reduction charge with the volume occupied by the p-type/n-type doping region and the elementary charge.

It is important to emphasize that the accuracy of the above doping-concentration calculation depends on the validity of the assumption that all the injected charge is consumed in electrochemical doping of the CP. It has previously been demonstrated that this assumption is invalid if the energy barrier for electrochemical p-type doping of the CP is different than that for electrochemical n-type doping (resulting in different amounts of charge stored in the electric double layers at the two electrode-active material interfaces).[24,60−61] However, it has also been demonstrated that this correction is negligible for wide-gap devices with inter-electrode gaps of the order of 1 mm,[58] and we therefore do not consider it further in this work.

Another source for error in the doping-concentration calculation is related to the fact that electrochemical reactions other than doping of the CP can take place in LECs, and we choose to collectively term such reactions as "electrochemical side-reactions". An important indication that these electrochemical side-reactions indeed take place in the herein-studied devices
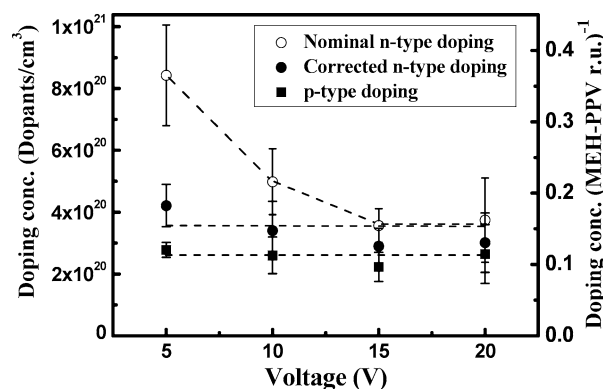

Figure 4. Average value and the associated error bar for the nominal n-type doping concentration (open circles), the corrected n-type doping concentration (solid circles), and the p-type doping concentration (solid squares) as a function of applied voltage. The data were calculated at the time of the initial p−n junction formation in planar Au/{MEH-PPV + PEO + KCF₃SO₃}/Au surface cells with a 1-mm inter-electrode gap. The dashed lines are a guide-to-the-eye.

is the delay in the n-type doping onset in comparison to the p-type doping onset clearly apparent in Figures 2 and 3. This observation would be in direct violation with the charge-conservation law, which dictates that electrochemical oxidation must be balanced by electrochemical reduction in an LEC during the turn-on process, unless an electrochemical side-reaction takes place at the cathodic interface, particularly during the time period at which solely p-type doping is observed.

Figure 4 presents the p-type doping concentration (solid squares) as calculated with the above method by integrating the current from the time of the p-type doping onset up to the time of the initial p−n junction formation. The n-type doping concentration was calculated using either the same time limit as above, yielding a "nominal n-type doping concentration" (open circles), or by integrating the current from the time of the onset of n-type doping to the time of the p−n junction formation yielding a "corrected n-type doping concentration" (solid circles). The latter approach is obviously more "correct", but it is important to point out that it is still based on one specific scenario, namely that electrochemical side-reactions dominate on the cathodic side up to the time at which n-type doping appears, after which n-type doping dominates. This assumption is, however, supported by the optical probing of the n-type doping front, since n-type doping is first completely undetectable but when the n-type doping front appears it grows in size quickly (see Figures 2 and 3). In this model, the extent of the side-reaction can be estimated by the difference between the nominal n-type doping concentration value and the corrected n-type doping concentration value.

It seems plausible that the observed transition in the preferred electrochemical reaction could originate in the chemical properties of the effective cathodic interface, and that the electrochemical side-reaction is preferred when the cathodic reaction takes place at the Au interface, but that n-type doping of MEH-PPV is preferred when the effective cathodic reaction front shifts to the front edge of the n-type doped MEH-PPV. We note that the inhibition of an electrochemical reaction by changing the chemical properties of the surface can be a common and useful feature, and that, e.g., a thin film of a doped conjugated polymer can effectively protect an underlying metal from corrosion.[62−64]

(53) Robitaille, C. D.; Fauteux, D. *J. Electrochem. Soc.* **1986**, *133*, 315−325.
(54) Marzantowicz, M.; Dygas, J. R.; Krok, F.; Florjancayk, Z.; Zygadlo-Monikowska, E. *J. Non-Cryst. Solids.* **2006**, *352*, 5216−5223.
(55) Henderson, W. A. *Macromolecules* **2007**, *40*, 4963−4971.
(56) Burns, S. E.; Greenham, N. C.; Friend, R. H. *Synth. Met.* **1996**, *76*, 205−208.
(57) McGehee, M. D.; Heeger, A. J. *Adv. Mater.* **2000**, *12*, 1655−1668.
(58) Shin, J. H.; Xiao, S.; Edman, L. *Adv. Funct. Mater.* **2006**, *16*, 949−956.
(59) Shin, J. H.; Matyba, P.; Robinson, N. D.; Edman, L. *Electrochim. Acta.* **2007**, *52*, 6456−6462.
(60) Edman, L.; Summers, M. A.; Burrato, S. K.; Heeger, A. J. *Phys. Rev. B.* **2004**, *70*, 115212.
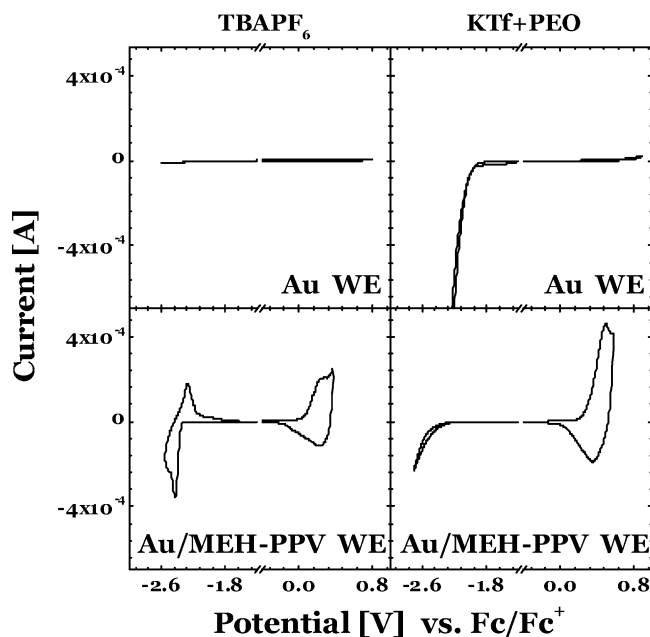(61) Buda, M.; Kalyuzhny, G.; Bard, A. J. *J. Am. Chem. Soc.* **2002**, *124*, 6090−6098.
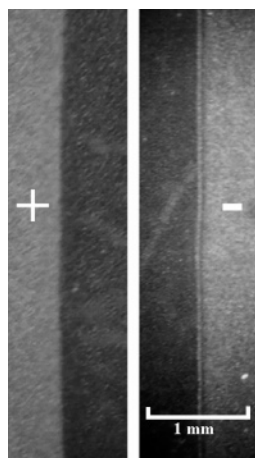
Figure 5. Optical microscopy images of the anodic (left) and cathodic (right) interfaces after ~12 h operation at $V = 30$ V and $T = 360$ K of a planar Au/{MEH-PPV + PEO + KCF$_3$SO$_3$}/Au surface cell with a 1-cm inter-electrode gap. The white line just to the left of the Au electrode on the right appears to be the product of a cathodic electrochemical side-reaction.

Returning to Figure 4, we find that both the p-type doping concentration and the corrected n-type doping concentration are essentially voltage-independent (see the two lower dashed lines in Figure 4). The p-type doping concentration is ~2.6×10^{20} dopants/cm^3, which corresponds to ~0.11 dopants/MEH-PPV repeat unit; and the corrected n-type doping concentration is ~3.5×10^{20} dopants/cm^3, which corresponds to ~0.15 dopants/ MEH-PPV repeat unit. The value for the p-type doping concentration is in good agreement with previous reports on similar devices, while the corrected n-type doping concentration is lower.[45,59] The discrepancy in the latter case is caused by the lack of correction for the delayed n-type doping onset in the earlier studies.

Our current interpretation of the voltage-independent doping concentration is that there is a specific doping value for which MEH-PPV exhibits a clear transition from a low- to a high-conductivity state, and that it is at this specific transitional doping value that the front progresses forward independent of the applied voltage. This conclusion is supported by a previous publication in which we demonstrated that the "overpotential" (defined as the applied potential subtracted by the band gap potential of the CP) is primarily dropping over the undoped region, and not at the interfaces or the doped regions, during device turn on.[44]

Direct visual evidence for an electrochemical side-reaction at the cathodic interface in devices which exhibit significant time difference between the onset of p-type and n-type doping is provided by optical microscopy images. Figure 5 shows the anodic interface (left) and the cathodic interface (right) of a planar Au/{MEH-PPV + PEO + KCF$_3$SO$_3$}/Au surface cell with an extremely large inter-electrode gap of 1 cm after long-term operation at $V = 30$ V. While the anodic interface retains a "clean" appearance after the long-term operation, a bright "degradation layer" has emerged at the cathodic interface between the negative Au electrode and the {MEH-PPV + PEO + KCF$_3$SO$_3$} active material. It is interesting to note that we,

(62) Wei, Y.; Wang, J. G.; Jia, X. R.; Yeh, J. M.; Spellane, P. *Polymer* **1995**, *36*, 4535−4537.
(63) de Souza, S. *Surf. Coat. Technol.* **2007**, *201*, 7574−7581.
(64) Kowalski, D.; Ued, M.; Ohtsuk, T. *Corros. Sci.* **2007**, *49*, 3442−3452.

Figure 6. Cyclic voltammetry data recorded using a working electrode (WE) of Au (top graphs) and Au coated with a thin film of MEH-PPV (lower graphs). The electrolyte solution was 0.1 M TBAPF$_6$ in CH$_3$CN (left graphs) and 0.1 M KCF$_3$SO$_3$ + 2 M PEO in CH$_3$CN (right graphs), respectively. A silver wire was used as the quasi-reference electrode, and it was calibrated vs the Fc/Fc$^+$ reference redox couple at the end of each measurement. The counter electrode was Pt, and the scan rate was 25 mV/s.

in general, find that the degradation layer is easiest to discern in devices that exhibit slow doping kinetics, i.e., devices operated at a low overpotential and/or low temperature (when the ionic conductivity of the active material is very low), and with large inter-electrode gaps. We will discuss why we believe this occurs later on in this work. We are also currently working with the identification of the products of the side-reaction, and we hope to be able to come back with these data in a later work.

Insight into the electronic structure of the various components in the LEC, i.e., the Au electrode, the MEH-PPV polymer, and the {KCF$_3$SO$_3$ + PEO} electrolyte, is provided by cyclic voltammetry (CV). Figure 6 shows CV data recorded employing either bare Au (top graphs) or Au coated with a thin film of MEH-PPV (lower graphs) as the working electrode, and using either TBAPF$_6$ in CH$_3$CN (left graphs) or {KCF$_3$SO$_3$ + PEO} in CH$_3$CN (right graphs) as the electrolyte solution. The top left graph demonstrates that the bare Au electrode is electrochemically inert in the probed voltage range (spanning between −2.6 V and +0.8 V vs the Fc/Fc$^+$ couple), while the lower left graph demonstrates that MEH-PPV can be reversibly n-type doped (reduced) at −2.3 V vs Fc/Fc$^+$ and reversibly p-type doped (oxidized) at +0.1 V vs Fc/Fc$^+$. (These redox values are ~0.1 V lower than those reported in a previous publication,[59] which we attribute to the different sources of the MEH-PPV polymer.) Importantly, when the electrolyte is changed from TBAPF$_6$ to {KCF$_3$SO$_3$ + PEO} the situation changes drastically in that a significant irreversible reduction reaction emerges in both the bare Au-electrode system (top right graph) and in the MEH-PPV-coated Au-electrode system (bottom right graph). On the basis of these data, we draw the conclusion that the {KCF$_3$SO$_3$ + PEO} electrolyte is irreversibly reduced at a lower potential than MEH-PPV is reversibly n-type doped.
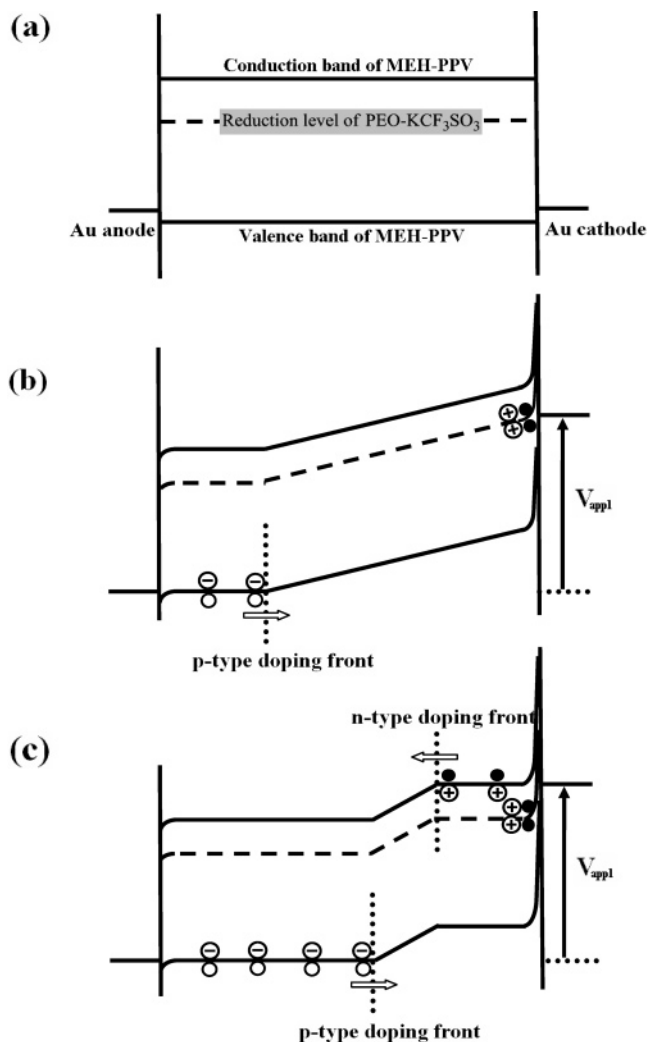
Figure 7. (a) Schematic electron-energy level diagram for an LEC, with the reduction level for the {KCF₃SO₃ + PEO} electrolyte positioned within the band gap of the (MEH-PPV) conjugated polymer (CP). The electronic and ionic response during (b) the "initial stage" operation, when the p-type doping of the CP at the anode is balanced by an electrochemical side-reaction of the electrolyte at the cathode, and during (c) the "later stage" operation, when the subsequent p-type doping is balanced by n-type doping. The larger circles represent ions, the smaller open and solid circles represent holes and electron, respectively, and the arrows represent electronic charge injection resulting in electrochemical doping. For clarity, the electric double layers at the interfaces are omitted.

Figure 7 presents the proposed operational mechanism of the LECs, in the form of a schematic electron-energy diagram. In agreement with the CV data, we include in Figure 7a a reduction level of the {KCF₃SO₃ + PEO} electrolyte at a lower energy than the conduction band edge of MEH-PPV (corresponding approximately to the n-type doping level). During the "initial stage" operation, as presented in Figure 7b, the electrochemical redox balance in the LEC is maintained by p-type doping (oxidation) of MEH-PPV at the anode and reduction of the electrolyte at the cathode. The latter reaction corresponds to the electrochemical side-reaction, which manifest itself in the lack of n-type doping progression during the initial stage operation (see Figures 2 and 3) and in the form of the degradation layer at the interface between the negative Au electrode and the active material (see Figure 5). During the "later stage" operation, the p-type doping at the anode is instead

balanced by n-type doping at the cathode, and it is during this process that n-type doping emerges in Figures 2 and 3.

An interesting question that deserves attention at this stage is related to the transition between the electrochemical-side reaction and the n-type doping at the Au cathode, and why it takes place earlier at higher applied voltage and/or increased ionic conductivity of the active material. We propose that the side-reaction is the thermodynamically preferred cathodic reaction (which is supported by the CV data), but that the n-type doping is the kinetically preferred cathodic reaction at the Au cathode interface. This has the consequence that when very little overpotential is available at small drive voltage or because all overpotential is dropping over a low-ionic conductance undoped region, the thermodynamically preferred side-reaction wins, since the n-type doping reaction simply is not energetically accessible. The situation changes at higher drive voltage or when the ionic conductance of the undoped region (separating the p-type and n-type regions) increases (because its ionic conductivity increases or because it decreases in size during later stages of the doping process) since there is then sufficient overpotential available at the cathodic interface to allow for both the side-reaction and n-type doping. In such a scenario, the kinetically favored reaction, the n-type doping, takes over. Moreover, as discussed previously, during this later-stage operation when the effective cathodic interface is located at the n-type doping front, and not at the Au electrode, the acquired data indicate that n-type doping is the dominant process.

Two directly apparent consequences of the electrochemical side-reaction are that the n-type doping onset is delayed and that the p−n junction shifts toward the cathode. One can also expect that the electrochemical side-reaction will produce reactant residues on the surface of the Au cathode (as visualized in Figure 5), which subsequently will at least partially block the initial n-type doping. The existence of a partial passivation layer on the Au cathode surface, but not on the Au anode surface, following the side-reaction is also consistent with the observation that the initial n-type doping front exhibits a spike-like appearance that is absent in the initial p-type front (see Figure 2). The existence of an insulating degradation layer between the negative Au electrode and the active material could also have implications for the voltage distribution in a turned-on LEC containing a light-emitting p−n junction, as it is reasonable to expect that it will cause a significant portion of the overpotential to shift from, e.g., the p−n junction to the degradation layer. We note that such behavior could have a notable influence on the results and conclusions inferred from scanning Kelvin probe measurements on planar surface-cell LECs.[65−66]

Conclusions

In order to improve upon the operation of LECs, it is important to minimize the extent of side-reactions and to form the light-emitting p−n junction in the center of the interelectrode gap. In this work, we demonstrate that an electrochemical side-reaction at the cathodic interface can be the dominant process during the initial operation of common LECs, as directly

(65) Slinker, J. D.; DeFranco, J. A.; Jaquith, M. J.; Silveira, W. R.; Zhong, Y. W.; Moran-Mirabal, J. M.; Craighead, H. G.; Abruna, H. D.; Marohn, J. A.; Malliaras, G. G. *Nat. Mater.* **2007**, *6*, 894−899.
(66) Pingree, L. S. C.; Rodovsky, D. B.; Coffey, D. C.; Bartholomew, G. P.; Ginger, D. S. *J. Am. Chem. Soc.* **2007**, *129*, 15903−15910.

evidenced by the formation a degradation layer at the cathodic interface and by a delay in the onset of n-type doping. We further show that it is possible to alleviate the extent of this undesired side-reaction, and attain a relatively centered p−n junction, by operating LECs at a high initial applied voltage and under conditions at which the LEC active material exhibits high ionic conductivity. We rationalize these findings with an electrochemical model in which the thermodynamically preferred cathodic reaction is the side-reaction, while the kinetically preferred reaction is n-type doping of MEH-PPV. Finally, we show that the doping concentrations in the doped regions at

the time of the p−n junction formation is essentially independent of the applied voltage at ∼0.11 dopants/ MEH-PPV repeat unit in the p-type region and ∼0.15 dopants/MEH-PPV repeat unit in the n-type region.